Excitation and Stability of Ultrahigh Rydberg States in Stray Electric Fields

Paolo Bellomo,*,†,§ David Farrelly,‡ and T. Uzer†

School of Physics, Georgia Institute of Technology, Atlanta, GA 30332-0430, and Department of Chemistry and Biochemistry, Utah State University, Logan, Utah 84332-0300

Received: June 13, 1997; In Final Form: September 10, 1997[⊗]

We demonstrate the feasibility of exciting long-lived, circular Rydberg states by time dependent weak electric fields such as might be encountered in typical ZEKE-PES (zero-electron-kinetic-energy photoelectron spectroscopy) conditions. Through a geometric interpretation of the dynamics, we identify the field configurations needed for either the stability or the excitation of ultra-long-living Rydberg states and conclude that nonuniform stray fields could be (partially) responsible for the observed, anomalously long lifetimes exhibited by ultrahigh Rydberg states, although under typical ZEKE-PES conditions other mechanisms like, for example, ion-Rydberg collisions constitute the main stabilization agent.

1. Introduction

Zero electron kinetic energy (ZEKE) spectroscopy is a robust and widely used method for obtaining spectra of molecular ions or clusters with laser-optical resolution.[1−8] The method relies on producing, and subsequently ionizing, ultrahigh, ultra-long-living molecular Rydberg states[9] ("ZEKE states") with principal quantum number $n \gtrsim 100$. An issue that has attracted considerable attention lately is the enhanced stability of such states.[10−16] It is generally accepted that ZEKE states are a superposition of angular momentum (l) eigenstates, in which the high-l states carry more weight than low-l ones. Therefore, the expectation value of the angular momentum over ZEKE states is large, and it is understood that ZEKE states owe their exceptional stability precisely to their large angular momentum. However, in this paper we focus directly on the dynamics of high-n, definite-l states in weak external fields. These states are an acceptable approximation to the long-lived ZEKE states which occur in the experiments; moreover the understanding of their dynamics opens the way to the accurate manipulation of ultrahigh, atomic, or molecular Rydberg states by applied, weak external fields. Therefore, from the standpoint of ZEKE the issue is how the initially small-l states, which are prepared in a few-photon experiment, are stabilized (i.e., how they acquire large angular momenta). Clearly, a number of mechanisms may be at work, and recently intramolecular stabilization mechanisms have also been proposed, in which the nature of the coupling between the rotation degrees of freedom of the core and the degrees of freedom of the Rydberg electron plays an important role.[14,15] However, collisions with neighboring ions,[12,13,16] which are always present in a molecular beam, are an effective way for the Rydberg electron to acquire a large angular momentum, and the effects of uniform dc fields[14] (if any are present) should be considered too. All these mechanisms must contribute, to a greater or lesser extent, to the excitation of long-lived ZEKE states. We concentrate here on the effects of one of the many agents which may contribute to the excitation of stable ZEKE states, i.e., *nonuniform*, weak, stray electric fields. In fact, under the most typical ZEKE experimental conditions, the initial small-l states are exposed, among other things, to weak, stray electric fields. In this article, we address two questions, namely how stray fields can excite large-l states and also how these large-l states are affected by weak electric fields.

The problem of the stability of such states in very weak electric fields is particularly interesting, because it is related to the intriguing observation that the lifetimes of ZEKE states do not scale as $\sim n^3$ as was expected by extrapolation from low-n quantum calculations based on hydrogenic approximations. The lifetimes observed in the experiments are much longer, probably scaling as as either $\sim n^4$ or $\sim n^5$.[1,10−13] However there is no clear experimental evidence yet of the exact n-dependence of the lifetimes of ZEKE states.[17−19] Most likely, the scaling with n of the lifetimes of ZEKE states is given by the convolution of more than one single power law and it depends on the specific experimental conditions.

It is clear that small-l states are necessarily shorter lived than large angular momentum states. For small angular momenta, the Rydberg electron is effectively coupled to the electronic cloud around the molecular core, which quickly leads to either autoionization of the electron or dissociation of the molecule. The matrix elements describing the process scale as $\sim n^{-3/2}$,[9] as one can see by applying first-order perturbation theory to the hydrogenic approximation, and become rapidly negligible for larger l's. Therefore, the lifetimes are expected to scale as $\sim n^3$ and also to be much longer for Rydberg states with large angular momenta.

Ultrahigh Rydberg states, however, are in an anti-Born−Oppenheimer[20] regime (the electron frequency is the slowest in the system, slower even than core rotation) and the quantum numbers involved are so large that classical (and semiclassical) methods give *quantitative* agreement with experiments[16] and full quantum treatments.[21] Moreover, a classical approach constitutes the most practical way of investigating the dynamics of these states, because the very high density of states (and also the large degeneracy, for large n's, of hydrogenic n-manifolds) means that the computational demands of an accurate quantum calculation escalate dramatically, posing formidable challenges to contemporary computers. In any case, classical mechanics leads to the same conclusions on the stability of large vs small angular momentum states: the expected scaling of the lifetimes of low-L (in this paper we indicate the classical angular momentum by L and the corresponding quantum number by l) classical orbits obeys the same $\sim n^3$ law as low-l quantum states. In the classical picture the Rydberg electron, being exposed to a potential which is almost exactly Coulombic, follows a Kepler ellipse[22] to a good approximation, and can exchange energy with the core electrons only when it is in the proximity of the molecular or atomic core i.e., once per orbit). The period of a Kepler orbit scales as $\sim n^3$,[22] which yields the same prediction for the scaling of the lifetimes of Rydberg electrons as a

† Georgia Institute of Technology.
‡ Utah State University.
§ Present Address: The Institute of Optics, University of Rochester, Rochester, New York, 14627-0186.
⊗ Abstract published in *Advance ACS Abstracts,* November 15, 1997.

S1089-5639(97)01931-2 CCC: $14.00

quantum mechanical analysis. Moreover, if the Rydberg electron moves along a large-L orbit, i.e., a Kepler ellipse with small eccentricity, then it senses a strong centrifugal barrier and it cannot approach the molecular core closely; therefore, energy exchanges with the core are quenched and the orbit becomes stable.

Since ultra-long-living ZEKE states are (in our approximation, as we will tacitly assume in the rest of the paper) Rydberg states with large angular momentum, a *mechanism* which can populate high-l Rydberg states will consequently enhance the ZEKE signal. It has been argued (and experiments confirm[14,17,18]) that weak dc fields increase the lifetimes of Rydberg states by mixing different angular momentum states. In the hydrogenic approximation, a small-l state, when placed in a uniform dc field, mixes with all the other $n - 1$ angular momentum states, and since the large-l states are stable, the probability of decay of the state becomes diluted by a factor $\sim n$. However, dc fields cannot change the magnetic quantum number m_l, because the projection of the angular momentum along the axis of the external field is a constant of motion, and high-l states carry the same weight as low-l states, despite their larger degeneracy ($g_l = 2l + 1$). Therefore, uniform, dc fields cannot account for all of the proposed extra $\sim n^2$ factor in the lifetimes.[12,13] On the other hand, weak fields with time dependent orientation can change m_l, and nonuniform stray fields[23] (as well as fields due to neighboring moving ions) are conjectured to be the cause of the unaccounted diffusion in m_l space. If m_l is not conserved, high-l states become statistically favored, and $\sim n^2$ stable states become available to the Rydberg electron, which leads to a greater dilution of the decay probability and to the extra $\sim n^2$ factor in the lifetimes. In this paper we examine the effect of stray electric fields of varying orientation on Rydberg states and answer the question of how and when they can significantly contribute to the extended lifetimes of ZEKE states. The strength of our study is that most of the results may be obtained analytically. The price we pay is that we restrict our analysis to a simple, but representative hydrogenic model. Indeed, our classical model captures the essence of the excitation and stabilization mechanism and we prefer to confine our study to this idealized problem reserving our study of dipolar and quadrupolar effects in alkali atoms for a another publication.[24] This paper is organized as follows. In section 2 we briefly review our classical model of the dynamics of Rydberg electrons in weak, slowly varying electric fields; in section 3 we present our explanation of the experimental results of Gross and Liang[21] and generalize their numerical results on the stability of very high-l states ("circular states"), providing a complete analysis of the dynamics of such states in weak, slowly varying electric fields. In the same section we also discuss the excitation of high-l ZEKE states by stray electric fields. We finally draw some general conclusions in section 4.

2. The Model

In this section we briefly review our classical model, which we described in detail elsewhere.[16] We begin our analysis by considering an uniform dc field (Stark effect). The corrections to the pure hydrogenic eigenenergies are linear in the field,[20] which means that physically the external field is coupled to the permanent electric dipole of the Rydberg state. Clearly, hydrogenic states do not have a permanent electric dipole moment in the usual $\{n,l,m_l\}$ basis, but the Hamiltonian of the hydrogen atom can also be diagonalized in parabolic coordinates,[20] and in that basis the eigenstates exhibit a permanent electric dipole moment. Classical mechanics provides a more intuitive picture of the origin of such dipole: the electron spends a much longer time at the aphelion of the Kepler orbit (see Figure 1), where it moves much more slowly, and its *average* charge distribution is therefore skewed toward the aphelion of the ellipse, thereby yielding a permanent electric dipole moment.[25−27] The Stark frequency[20] ω_S (in atomic units, which we use throughout this paper, $\omega_S = {}^3/_2 n\mathbf{F}$, where $\mathbf{F}$ is the external field) of typical, weak stray fields ($\mathbf{F} \sim 5$ V/m) is usually much smaller than the Kepler frequency,[22] $\omega_K = n^{-3}$, of the Rydberg electron. This means that the electron revolves around the Kepler orbit many times before the external field can change the angular momentum of the electron significantly. Under such conditions the Kepler orbit itself can be treated as a dynamical object,[21,25,26] in the sense that the parameters which determine the characteristics of the ellipse change in time, and precisely those parameters become the dynamical variables of the motion. Essentially, by a direct application of classical perturbation theory, we study the effects of the external field on the *elements* (in the sense of celestial mechanics[28]) of the Kepler ellipse. Also, if the Stark frequency is larger than the precession frequency due to the quantum defect (this is generally satisfied if $l_{\text{Rydberg}} > l_{\text{core}}$, where l_{core} is the largest possible angular momentum of the core electrons), the analysis of the hydrogenic model not only encapsulates the dominant dynamics[14,16,17,29] but is also capable of providing a *quantitative* explanation of the experimental results.[19,30] The dynamical variables of the model are the angular momentum $\mathbf{L}$ and the Runge−Lenz vector $\mathbf{A}$ of the orbit,[22] which fully describe a Kepler ellipse. The angular momentum is orthogonal to the plane of the ellipse and also defines the sense of the motion along the orbit, while the Runge−Lenz vector points in the direction of the perihelion and its magnitude is equal, in atomic units, to the eccentricity of the ellipse. The equations of motion, however, turn out to be particularly simple when expressed in terms of the *scaled* Runge−Lenz vector $\boldsymbol{a} = n\boldsymbol{A}$, which has the dimensions of an angular momentum, is obviously orthogonal to $\mathbf{L}$ and satisfies a constraint equation with it:

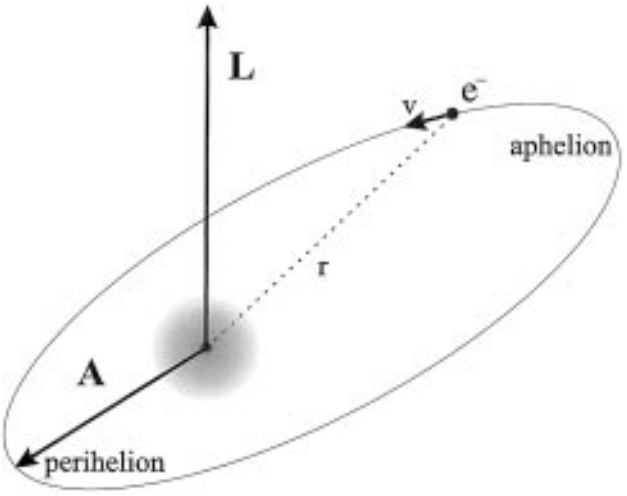

Figure 1. A Kepler ellipse and the two orthogonal conserved vectors, the angular momentum $\mathbf{L}$ and the Runge−Lenz vector $\mathbf{A}$ (not to scale): these two vectors define uniquely both the shape of the Kepler ellipse and its orientation in space and also the sense of the motion of the Rydberg electron along the orbit.

$$L^2 + a^2 = n^2 \tag{1}$$

Note that the scaled Runge−Lenz vector may range between 0 and n, just like the angular momentum of a Rydberg electron in an n-manifold, so that we may speak of "large" or "small" $\mathbf{a}$'s in the same sense in which we speak of "large" or "small" angular momenta. It is next convenient to introduce two new vectors, which are simple combinations of $\mathbf{L}$ and $\mathbf{a}$ and are the

generators of SO(4) (i.e.,

$$\boldsymbol{\xi} = {}^1/_2\,(\mathbf{L} + \mathbf{a}) \tag{2}$$

$$\boldsymbol{\eta} = {}^1/_2\,(\mathbf{L} - \mathbf{a})$$

The equations of motion of $\boldsymbol{\xi}$ and $\boldsymbol{\eta}$ are particularly simple:

$$\frac{\mathrm{d}\boldsymbol{\xi}}{\mathrm{d}t} = -\,\boldsymbol{\omega}_\mathrm{S} \times \boldsymbol{\xi} \tag{3}$$

$$\frac{\mathrm{d}\boldsymbol{\eta}}{\mathrm{d}t} = \boldsymbol{\omega}_\mathrm{S} \times \boldsymbol{\eta}$$

where ω_S is the Stark frequency mentioned before. Not surprisingly, eqs 3 were derived originally by Born.[26] The solution of these equations is easy in the case of a time independent external field: in that case the two vectors $\boldsymbol{\xi}$ and $\boldsymbol{\eta}$ simply precess, clockwise and counterclockwise respectively, around ω_S, as was pointed out already by Percival.[27] In typical experimental settings, however, Rydberg atoms or molecules travel in a beam and they sense any spatially nonuniform field as a *time dependent field*, which makes the dynamics more complicated. To a first approximation, however, a time varying stray field can be modeled by a field rotating uniformly (around the *y*-axis) with frequency ω_R,[21] i.e., a circularly polarized (CP) field:

$$\mathbf{F} = \mathrm{F}\,[\cos(\omega_\mathrm{R}t)\hat{\mathbf{k}} + \sin(\omega_\mathrm{R}t)\hat{\mathbf{i}}] \tag{4}$$

Gross and Liang[21] studied the special case of the stability of very high-*l* states under the action of the field in eq 4). This seemingly idealized problem reveals interesting clues about the stability of circular Rydberg states in time dependent, weak electric fields. Gross and Liang, however, confined themselves to the case in which **L** is initially aligned with the external field and integrated eqs 3 numerically; their results agree well with their full quantum treatment (showing that for very large *n*'s eqs 3) are very accurate, whereas the computational demands of a quantum treatment escalate dramatically). Those authors also checked their results experimentally, thus verifying the accuracy of the classical predictions and quantum calculations.

The emphasis of the work in ref 21 was on the study of the stability of high-*l* states, and their results, both numerical and experimental, show that for slowly varying fields the long-living circular states remain essentially circular, if the angular momentum of the Rydberg electron is initially aligned with the external field. We reproduced their calculations and we show the results in Figure 2], where curves a, b, and c are essentially identical with the plots in ref 21. It is clear that very different dynamical behaviors are possible (see Figure 2). We can explain the dynamics analytically and our approach can also make sense of the strange trajectory of curve d, so that, in what follows, we explain and also *generalize* the results of ref 21.

3. Results

It is convenient to treat the problem of a Rydberg electron in a rotating electric field by viewing the dynamics in a frame rotating with the field, so that in the new frame the field (and therefore also the Stark frequency ω, associated with it) becomes a time independent field. It is also useful to observe that since the field in eq 4 rotates in the $\{x,z\}$-plane, the axis of rotation is directed along the *y*-axis and it is also time independent both in the inertial and rotating frame. By transforming to the rotating frame the following operator equation holds[22]

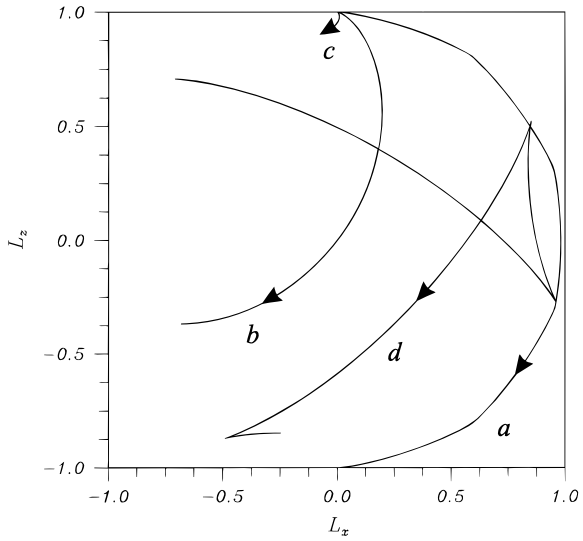

Figure 2. These curves show how **L** responds to the action of a weak electric field **F** rotating with frequency ω_R. **F** and **L** are initially aligned along the *z* -axis, and the evolution of the projection of **L** onto the $\{x,z\}$-plane is shown for up to a time $t = \pi/\omega_\mathrm{R}$. Curves a, b, c, and d, correspond to $\omega_\mathrm{S}/\omega_\mathrm{R} = 10$, 1, 0.2, and 10 again (but with a different initial angle between **L** and the field), respectively. The magnitude of **L** is normalized to 1.

$$\left(\frac{\mathrm{d}}{\mathrm{d}t}\right)_\mathrm{rotating} = \left(\frac{\mathrm{d}}{\mathrm{d}t}\right)_\mathrm{fixed} - \boldsymbol{\omega}_\mathrm{R} \times \tag{5}$$

and the equations of motion become

$$\frac{\mathrm{d}\boldsymbol{\xi}}{\mathrm{d}t} = -(\boldsymbol{\omega}_\mathrm{S} + \boldsymbol{\omega}_\mathrm{R}) \times \boldsymbol{\xi} \tag{6}$$

$$\frac{\mathrm{d}\boldsymbol{\eta}}{\mathrm{d}t} = (\boldsymbol{\omega}_\mathrm{S} - \boldsymbol{\omega}_\mathrm{R}) \times \boldsymbol{\eta}$$

where $\omega_\mathrm{R}\hat{\mathbf{j}}$. These equations can be solved analytically, by introducing the propagators for $\boldsymbol{\xi}$ and $\boldsymbol{\eta}$ respectively, so that the time evolution is given by

$$\boldsymbol{\xi}(t) = U^{+}_\mathrm{rot}\,(t,t')\boldsymbol{\xi}(t') \tag{7}$$

$$\boldsymbol{\eta}(t) = U^{-}_\mathrm{rot}\,(t,t')\boldsymbol{\eta}(t')$$

Introducing the precession frequency ω and the total angle of precession ϕ as

$$\omega = \sqrt{\omega_\mathrm{S}^2 + \omega_\mathrm{R}^2} \tag{8}$$

$$\phi = \omega(t - t')$$

the exact propagators in the rotating frame are[16]

$$U^{\pm}_\mathrm{rot}(t,t') = \begin{pmatrix} \cos\phi & \pm\dfrac{\omega_\mathrm{S}}{\omega}\sin\phi & -\dfrac{\omega_\mathrm{R}}{\omega}\sin\phi \\ \mp\dfrac{\omega_\mathrm{S}}{\omega}\sin\phi & \dfrac{\omega_\mathrm{S}^2}{\omega^2}\cos\phi + \dfrac{\omega_\mathrm{R}^2}{\omega^2} & \pm\dfrac{\omega_\mathrm{S}\omega_\mathrm{R}}{\omega^2}[1 - \cos\phi] \\ \dfrac{\omega_\mathrm{R}}{\omega}\sin\phi & \pm\dfrac{\omega_\mathrm{S}\omega_\mathrm{R}}{\omega^2}[1 - \cos\phi] & \dfrac{\omega_\mathrm{R}^2}{\omega^2}\cos\phi + \dfrac{\omega_\mathrm{S}^2}{\omega^2} \end{pmatrix} \tag{9}$$

where the upper and lower signs of eq 4 give the propagators for $\boldsymbol{\xi}$ and $\boldsymbol{\eta}$, respectively. However, the exact, complicated form of the propagators in eq 9 is not particularly useful in providing *physical insight* into the dynamics and in identifying the

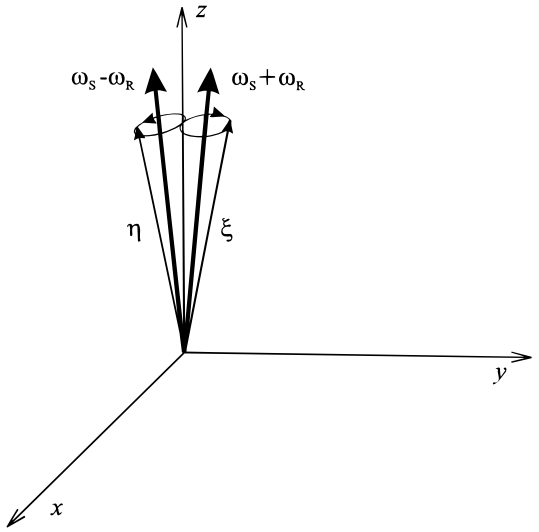

Figure 3. Trajectories of $\boldsymbol{\xi}$ and $\boldsymbol{\eta}$ in the rotating frame; $\omega_S/\omega_R = 10$. Both vectors precess on two narrow cones, shown in the figure, which have almost coincident axes, and therefore $\boldsymbol{\xi}$ and $\boldsymbol{\eta}$ never separate much, so that the state remains circular.

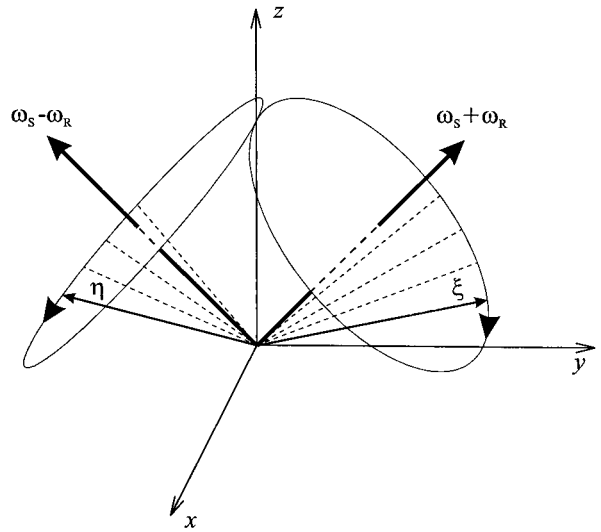

Figure 4. Trajectories of $\boldsymbol{\xi}$ and $\boldsymbol{\eta}$ in the rotating frame; $\omega_S/\omega_R = 1$. The two cones of the previous figure are no longer aligned, and the axes of precession have significant components along ω_R. $\boldsymbol{\xi}$ and $\boldsymbol{\eta}$ are still initially aligned with **F** (i.e., the *z*-axis of the figure, so that the amplitude of the precession cones becomes much larger than in the previous case.

mechanism behind the process. We prefer to present here a clear, *geometric* view of the motion which not only explains the numerical and experimental results of ref 21 at the *intuitive* level, but also allows us to estimate the conditions under which nonuniform stray fields become important in the excitation of ZEKE states. One can best understand the dynamics of $\boldsymbol{\xi}$ and $\boldsymbol{\eta}$ in the inertial frame by observing that it consists of of two components: a pair of precessions around different axes, which yields the dynamics in the rotating frame, and a rotation around the *y*-axis, which maps the two vectors back to the inertial frame. It is worth spending a few lines to clarify the relationship between $\boldsymbol{\xi}$ and $\boldsymbol{\eta}$ and the angular momentum, and therefore also the stability and lifetime, of Rydberg states. A small-*l*, short-lived state corresponds to the two vectors $\boldsymbol{\xi}$ and $\boldsymbol{\eta}$ being almost opposite, because $\boldsymbol{L} = \boldsymbol{\xi} + \boldsymbol{\eta}$. On the other hand, a large-*l*, long-lived state will be excited if, during their motion, $\boldsymbol{\xi}$ and $\boldsymbol{\eta}$ approach each other, and become approximately parallel (i.e., if their difference **a** becomes small, since the magnitude of **a**, which is proportional to the eccentricity of the orbit, is connected to the magnitude of **L** by eq 1). Finally, a circular, stable state remains (quasi) circular if the difference $\boldsymbol{a} = \boldsymbol{\xi} - \boldsymbol{\eta}$ remains small throughout the motion. We will consider three typical cases. First, when $\omega_R \ll \omega_S$, the two axes of precession are very close Figure 3]); if **L** is initially close to its maximum value (circular state) and originally aligned with the field, as in the experiments of Gross and Liang,[21] then $\boldsymbol{\xi}$ and $\boldsymbol{\eta}$ are initially almost parallel and they are also oriented approximately along the Stark frequency vector $\boldsymbol{\omega}$. During their motion $\boldsymbol{\xi}$ and $\boldsymbol{\eta}$ describe two cones of small amplitude, so that they are never distant from their own axes of precession which are almost coincident (see Figure 3): therefore $\boldsymbol{\xi}$ and $\boldsymbol{\eta}$ *do not separate significantly during their precession* and the state remains essentially circular. The rotation around $\hat{\mathbf{j}}$ simply reverses the direction of **L**, at the same rate of rotation as the external field, so that the angular momentum **L** tracks the **F**-vector, as is shown in curve a of Figure 2. This analysis provides a simple, intuitive explanation of both the numerical result and the experimental observation that under these conditions circular states maintain their circularity while the direction of the angular momentum is reversed.[21] A moment's thought shows that, by the same geometrical argument, a small **L**, large **a** state will follow a similar dynamics. A small **L** state, in which the scaled Runge−Lenz vector is initially aligned with a slowly rotating field, does not acquire a large angular momentum, while the scaled Runge−Lenz vector remains maximal and tracks the rotating electric field. These special results, however, depend on the choice of the initial conditions and a completely different outcome ensues from a different initial orientation of **L** (Figure 2, curve d, which could also be explained, albeit in a more complicated way, by the same approach). Therefore, we are able to conclude that the stability of circular states observed in ref 21 is strictly contingent to the initial orientation of the angular momentum relative to the external field.

Notice that the dynamics of Figure 2, curve a, and Figure 3 seems to contradict our statement that the external fields couple with the permanent electric dipole moment of the Rydberg orbit. Although the corrections to the energy levels of a hydrogen atom in an external electric field (Stark effect) can be calculated exactly by considering the *classical* energy shift due to an electric dipole in a dc field[20,25] and quantizing the Runge−Lenz vector, the dynamics of Figures 2 and 3 is not the same as for an electric dipole in a rotating external field. The effective electric dipole of a Kepler ellipse is oriented along **a**, which is always orthogonal to the angular momentum, so that the initial configuration in which the angular momentum and the field are aligned is a configuration of unstable equilibrium for the dipole (orthogonal to the field, which is a hyperbolic point[31]). As the electric field begins to rotate, one expects the dipole to move away from the hyperbolic point and to oscillate around the equilibrium point, namely, in alignment with the slowly rotating electric field. This, however, does not happen: the dipole rotates with approximately the same frequency as the field and remains essentially orthogonal to it. The reason for this unexpected dynamical behavior is that the effective dipole of the orbit of a Rydberg electron does not have any inertia term. Therefore, although the dipole analogy explains well the shift of the energy levels, the equations of motion are intrinsically different from the one of a real, physical dipole in a time dependent electric field, and new dynamical behavior appears, like curve a in Figure 2.

Next, consider the case in which $\omega_R \sim \omega_S$ Figure 4: now the two axes of precession are well separated, and no longer aligned with the *z*-axis; therefore, $\boldsymbol{\xi}$ and $\boldsymbol{\eta}$, although initially aligned with one another, describe two cones of large amplitude and drift apart during their motion. This implies that the eccentricity of the orbit grows and the state loses its circularity

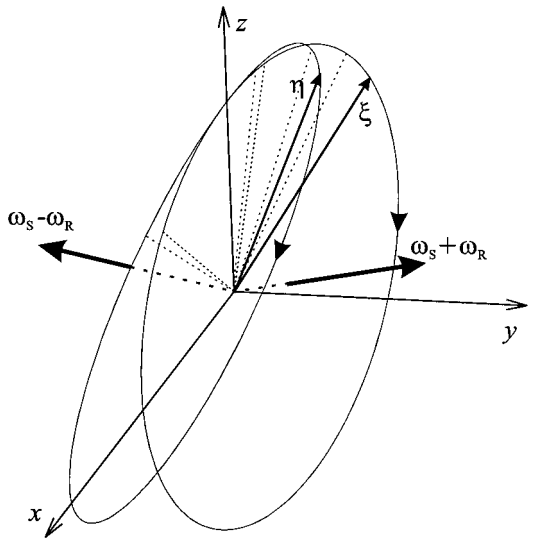

Figure 5. Trajectories of $\boldsymbol{\xi}$ and $\boldsymbol{\eta}$ in the rotating frame; $\omega_S/\omega_R = 0.2$. The two precession cones are now almost opposite and they have become very large, almost degenerating to a pair of disks; $\boldsymbol{\xi}$ and $\boldsymbol{\eta}$ point initially along the *z*-axis (i.e., they are initially almost orthogonal to their axes of precession).

Figure 2, curve b). The final result, after half a period, $^1/_2T_R$, depends strongly upon the ratio between ω and ω_R, as resonant effects become dominant, since $\boldsymbol{\xi}$ and $\boldsymbol{\eta}$ can eventually come together again.[16] Obviously the rotation around $\hat{\mathbf{j}}$, which maps all variables back into the inertial frame, does not influence the dynamics of the magnitudes of **L** and **a**. Finally we consider the limit in which $\omega_R \gg \omega_S$ Figure 5: in this case the two axes of precession are determined essentially by ω_R and are almost opposite to each other. However, $\boldsymbol{\xi}$ precesses clockwise because of the minus sign in eq 6 while $\boldsymbol{\eta}$ precesses counterclockwise so that the two vectors, which now describe almost a pair of back-to-back disks, remain very close to each other during their precessions and the state remains essentially circular. Also, $\omega \sim \omega_R$, and therefore the rotation around ω is almost exactly balanced by the precession around $\boldsymbol{\omega}$, so that also the direction of **L** remains essentially unchanged. This explains curve c in Figure 2 and was also observed experimentally.[21] We have so far clarified the problem of one of the two issues relevant to ZEKE, namely, the stability of circular states in weak, time dependent electric fields, and we have demonstrated that the stability of such states in slowly rotating fields, which was observed in the experiments[21] depends on the initial, relative orientation of the angular momentum and the external field. We will now show that our analysis of the results in ref 21, thanks to its greater generality, sheds some light also on the excitation of ZEKE states. In fact, in contrast with the first two cases, our argument for the stability of circular states when $\omega_R \gg \omega_S$ applies to *all* possible initial conditions, not only to the special case of circular states with **L** initially oriented along the field. This *generalizes* the results by Gross and Liang,[21] and applies to initial conditions with small *l*, which constitute the second issue relevant to ZEKE, namely how small-*l* states acquire large angular momenta. As we mentioned before, several mechanisms are at work, and we concentrate here on the role played by nonuniform stray fields.

It is clear that in the situation of Figure 5, the relationship between $\boldsymbol{\xi}$ and $\boldsymbol{\eta}$ does not vary significantly as the two vectors rotate around their respective axes of precession, *regardless of their initial configuration*. We conclude that the properties of *all* Rydberg states do not change significantly in a relatively rapidly varying, weak external field (as long as the conditions under which the model remains a good approximation are satisfied[16]). Our analysis also makes clear that the relevant parameters are not the absolute value of the field strength and rotation frequency as separate quantities, but rather their ratio, which determines the relative orientation of the axes of precession, in the rotating frame, for $\boldsymbol{\xi}$ and $\boldsymbol{\eta}$.[19,30] This key observation allows us to derive some estimates of the conditions under which nonuniform stray fields can or cannot significantly enhance the lifetimes of Rydberg states. Remember that Rydberg electrons are usually prepared by a laser pulse, and are initially in a small angular momentum state, due to the usual selection rules and if such electrons can be promoted to large-*l* states, they will avoid close collisions with the core, which are responsible for the decay of Rydberg states via either autoionization of the electron or dissociation of the molecule. A weak dc field can only change *l*, because in a Stark field the projection of **L** along the field is a constant of motion. Therefore, only one value of the magnetic quantum number is accessible and low-*l* and large-*l* states are equally probable, and, as we discussed before, a uniform distribution in *l* space can account only for an extra factor $\sim n$ in the lifetimes. However, we have shown (curves b and d in Figure 2 that fields with time dependent orientation *do change* m_l: an uniform distribution in m_l space greatly favors large-*l* states, thanks to the $2l + 1$ degeneracy factor; this in turn makes collisions with the core even less likely and provides a dynamical mechanism which accounts for the proposed $\sim n^2$ factor in the scaling of the lifetimes of ZEKE states.[12,13,16] In a typical ZEKE experiment, the atoms or molecules whose spectra are being investigated undergo a supersonic free jet expansion and then travel in a well collimated beam. Clearly, these atoms or molecules which are rapidly moving in the experimental beam, will sense any *nonuniform* stray field present in the experimental apparatus as a *time dependent* field. While a realistic stray field is not the same as a CP field, the analysis above can nevertheless give some useful results. Any time dependent field can be decomposed in a Fourier series, and each Fourier component contributes independently to the total transition matrix element (neglecting interference effects). We may then concentrate on the "typical" Fourier component of a stray field and study the effects of a field that rotates with that frequency. In fact, this is exactly the case of the field configuration studied experimentally by Gross and Liang:[21] those authors obtain good agreement between theoretical predictions and experimental results, even if the CP field of eq 4 is only an approximation to the actual field which they used in the experiments. The typical period of a CP field approximating a nonuniform stray field field should be equal to the ratio between the spatial correlation length λ of the stray field to be modeled, and the speed v of the supersonic molecular beam, so that we may consider a typical field frequency to be

$$\omega_R^{\text{Typical}} \sim \frac{2\pi v}{\lambda} \tag{10}$$

The condition under which a rotating field can change m_l effectively and excite the highest-*l* states is that the rotation frequency is not much larger than the Stark frequency of the field, namely,[16]

$$\frac{\omega_S}{\omega_R} \gtrsim {}^1/_2 \Rightarrow \lambda \gtrsim \frac{2\pi v}{3nF_{\text{stray}}} \tag{11}$$

At the same time, λ cannot be too large, otherwise the field will become almost uniform: this leads to the requirement that

$$\lambda \lesssim v\tau \tag{12}$$

where τ is a time shorter than the delay between the laser excitation of the Rydberg state, and the pulsed electric field

which ionizes the Rydberg molecules or atoms, and also collects the ionizing electrons which constitute most of the ZEKE signal. Typically, such delay is $\sim$1 μs,[32] and one may reasonably set $\tau \approx 100$ ns. Using typical values of the other experimental parameters,[32] namely $v \sim 1000$ m/s and $F_{\text{stray}} \sim 5$ V/m the two conditions yield

$$\frac{10^8}{n} \lesssim \lambda \lesssim 2 \times 10^6 \tag{13}$$

It follows that for $n \gtrsim 50$ there is scope for nonuniform stray fields to enhance Rydberg states lifetimes. Clearly, a shorter τ would imply a higher constraint on principal quantum number *n*. However, ZEKE experiments are performed exciting Rydberg states with principal quantum numbers which do satisfy the condition $n \gtrsim 50$ (in typical experiments, *n* is often much greater than such lower limit); therefore, nonuniform stray fields constitute a *viable* mechanism for the excitation of long-lived, high-*l* states, and *may* have been playing a nonnegligible role in the success of ZEKE. Under typical experimental conditions, stray fields are thought to be rather uniform, and they are probably not the most important agent in the stabilization process, in which many other mechanisms are involved; however, we have just shown that they cannot be totally neglected. In fact, typical ZEKE molecular beams also contain ions which move at a speed $\sim \delta v$ relative to the Rydberg atoms or molecules, where δv is the spread in the distribution of beam speeds. Since for typical experimental settings $\delta v \ll {}^1/_n$ ion-Rydberg collisions become tremendously effective in extending Rydberg lifetimes because of the very large cross section of slow $\{nl\} \rightarrow \{nl'\}$ collisions.[16] Recent experiments[18] were aimed at determining the mechanism of the enhancement of Rydberg lifetimes and great care was taken in reducing stray fields; in these experiments, in which extra ions were injected in the interaction region and long lifetimes were observed, indicate that ionic fields are indeed an important mechanism for lifetime enhancement. These results, however, do not necessarily contradict our analysis, which relates to *typical* ZEKE conditions, in which the goal of the experiment is a really the spectroscopic measurement and no special effort is made in reducing stray field beyond a reasonable value (and indeed we argue that it *should not be done*, since such fields may well contribute to the excitation of the useful, long-lived ZEKE states).

4. Conclusions

In this paper we have developed an analytic interpretation of so far unexplained, merely numerical and, most importantly, experimental results[21] on the stability of circular Rydberg states in time dependent, vanishing electric fields. Moreover, we have also derived a geometric and intuitive picture of the dynamics, which uncovers the mechanism for the stability of large-*l* states, and shows that the stability of such states, which was observed in the experiments,[21] is contingent to the specific, initial orientation of the angular momentum of the state relative to the external field. By the same approach, we have derived an estimate of the principal quantum numbers of Rydberg states beyond which, in the hydrogenic approximation, nonuniform stray electric fields *may* become effective in the excitation of ultra-long-living ZEKE states, which are the reason for the success of ZEKE−PES as a spectroscopic technique. Our conclusions on the role of nonuniform stray fields could be tested experimentally by measuring the *n*-dependence of the lifetimes of Rydberg states around the critical value $n_c \sim 50$ in a *ion free environment*. However, the role of the quantum defect should be first quenched by a microwave field,[16] so that the hydrogenic model would become more accurate. We expect that nonuniform stray fields should be able to enhance Rydberg lifetimes for sufficiently large *n*'s, and that long lifetimes should be observable even in ion free environments. Finally, our work, thanks to the clear geometric picture of the dynamics, suggests a simple way to prepare specific angular momentum states, in the quasidegenerate *n*-manifold, by selecting both the appropriate configuration of external fields and the time during which the Rydberg electron is exposed to such fields. In fact, a Rydberg electron in a weak, CP electric field in the rotating frame is equivalent to a Rydberg electron in crossed electric and magnetic field[33,34] in the inertial frame, as long as the magnetic field is weak enough (i.e., the rotation frequency of the CP electric field is small), and the diamagnetic term, which is quadratic in the field, can be neglected.

Acknowledgment. We thank Dr. Marc Vrakking for useful information about experimental parameters used in the measurements of Rydberg lifetimes. This work was partially supported by NSF and the donors of the Petroleum Research Fund, administered by the American Chemical Society.

References and Notes

(1) White, M. G. In *Frontiers of Chemical Dynamics*; Yurtsever, E., Ed.; Kluwer Academic Publishers: Dordrecht, 1995; p 43.
(2) Müller-Dethlefs, K.; Sander, M.; Schlag, E. *Z. Naturforsch. A* **1984**, *39*, 1089.
(3) Müller-Dethlefs, K.; Schlag, E. *Annu. Rev. Phys. Chem.* **1991**, *42*, 109.
(4) Müller-Dethlefs, K.; Schlag, E.; Grant, E.; Wang, K.; McKoy, B. *Adv. Chem. Phys.* **1995**, *90*, 1.
(5) Fischer, I.; Linder, R.; Müller-Dethlefs, K. *J. Chem. Soc., Faraday Trans.* **1994**, *90*, 2425.
(6) Müller-Dethlefs, K.; Dopfer, O.; Wright, T. G. *Chem. Rev.* **1994**, *94*, 1845.
(7) Schlag, E.; Peatman, W.; Müller-Dethlefs, K. *J. Electron Spectrosc. and Relat. Phenom.* **1993**, *66*, 139.
(8) Merkt, F.; Softley, T. P. *Int. Rev. Phys. Chem.* **1993**, *12*, 205.
(9) Gallagher, T. F. *Rydberg Atoms;* Cambridge University Press: Cambridge, 1994.
(10) Müller-Dethlefs, K. *J. Chem. Phys.* **1991**, *95*, 4821.
(11) Reiser, G.; Habenicht, W.; Müller-Dethlefs, K.; Schlag, E. W. *Chem. Phys. Lett.* **1988**, *152*, 119.
(12) Chupka, W. A. *J. Chem. Phys.* **1993**, *98*, 4520.
(13) Chupka, W. A. *J. Chem. Phys.* **1993**, *99*, 4580.
(14) Rabani, E.; Levine, R. D.; Mühlpfordt, A.; U. Even. *J. Chem. Phys.* **1995**, *102*, 1619.
(15) Farrelly, D.; Lee, E.; Uzer, T. *Phys. Lett. A* **1995**, *204*, 359.
(16) Bellomo, P.; Farrelly, D.; Uzer, T. *J. Chem. Phys.* **1997**, *107*, 2499.
(17) Vrakking, M. J. J.; Lee, Y. T. *J. Chem. Phys.* **1995**, *102*, 8818.
(18) Vrakking, M. J. J.; Lee, Y. T. *J. Chem. Phys.* **1995**, *102*, 8833.
(19) Jones, R. R.; Fu, P.; Gallagher, T. F. *J. Chem. Phys.* **1997**, *106*, 3578.
(20) Bethe, H. A.; Salpeter, E. E. *Quantum Mechanics of One- and Two-Electrons Atoms;* Plenum: New York, 1977.
(21) Gross, M.; Liang, J. *Phys. Rev. Lett.* **1986**, *57*, 3160.
(22) Goldstein, H. *Classical Mechanics*, 2nd ed.; Addison-Wesley: Reading, 1980.
(23) Merkt, F.; Zare, R. N. *J. Chem. Phys.* **1994**, *101*, 3495.
(24) Bellomo, P.; Farrelly, D.; Uzer, T. *Classical Theory of Collisional Intrashell Transitions in Alkali Rydberg Atoms*; 1998; to be published.
(25) Hezel, T. P.; Burkhardt, C. E.; Ciocca, M.; He, L.-W.; Leventhal, J. J. *Am. J. Phys.* **1992**, *60*, 324.
(26) Born, M. *Mechanics of the Atom;* Bell: London, 1960.
(27) Percival, I. C. In *Atoms in Astrophysics*; Burke, P. G., Eissner, W. B., Hummer, D. G., Percival, I. C., Eds.; Plenum: New York, 1983; p 75.
(28) Szebehely, V. *Theory of Orbits;* Academic Press: New York, 1967.
(29) Hezel, T. P.; Burkhardt, C. E.; Ciocca, M.; He, L.-W.; Leventhal, J. J. *Am. J. Phys.* **1992**, *60*, 329.
(30) Bellomo, P.; Farrelly, D.; Uzer, T. *Anomalous Autoionization Lifetimes of Rydberg States in a Circularly Polarized Microwave Field*; 1998, in press.
(31) Lichtenberg, A. J.; Lieberman, M. A. *Regular and Stochastic Motion;* Springer-Verlag: New York, 1983.
(32) Vrakking, M. J. J. Private Communication.
(33) von Milczewski, J.; Diercksen, G. H. F.; Uzer, T. *Phys. Rev. Lett.* **1994**, *73*, 2428.
(34) von Milczewski, J.; Diercksen, G. H. F.; Uzer, T. *International Journal of Bifurcation and Chaos* **1994**, *4*, 905.